High-Energy Heavy-Ion Irradiation Effects in Makrofol-KG Polycarbonate and PET

R. C. Ramola,[1] Ambika Negi,[1] Anju Semwal,[1] Subhash Chandra,[1] J. M. S. Rana,[1] R. G. Sonkawade,[2] D. Kanjilal[2]

[1]*Department of Physics, HNB Garhwal University, Badshahi Thaul Campus, Tehri Garhwal 249199, India*
[2]*Inter University Accelerator Centre, Aruna Asaf Ali Marg, New Delhi 110067, India*

ABSTRACT: This experimental study investigated the modification of optical, structural and morphological properties of Makrofol-KG and Polyethylene Terephtalate (PET) by irradiation of 120 MeV Ni^{+9} ions at fluences ranging from 1×10^{10} to 1×10^{12} ion/cm^2. Optical and structural properties were studied by UV–visible spectroscopy and X-ray diffraction (XRD) method, respectively. XRD studies of pristine and irradiated polymers revealed that crystallinity decreased after irradiation with swift heavy ions. The UV–visible spectrum displayed a shift in absorbance edge toward higher wavelength at higher fluence, which can be correlated with transition involved in polymers. Fourier transform infrared spectroscopy spectra were analyzed to investigate the changes in the chemical/structural properties of these polymers. The Makrofol-KG is found to exhibit more pronounced modification compared to PET after irradiation by swift heavy ions. The surface morphology studied by atomic force microscopy showed that the roughness of polymers surface increased with increasing fluence. © 2011 Wiley Periodicals, Inc. J Appl Polym Sci 121: 3014–3019, 2011

**Key words:** makrofol-KG polycarbonate; PET; ion beam; XRD; UV-visible; FTIR; AFM

INTRODUCTION

High-energy ion bombardment induced modifications in polymeric materials constitute an interesting and involved field of research. The swift heavy ions (SHI) at velocity of the order of Bohr velocity lose their energy mainly via electronic excitation and ionizations. The deposited energy gets converted into atomic motion and finally leads to several structural and chemical modifications within a cylindrical zone of a few nanometers in diameter.[1–4] Polycarbonates such as Makrofol are insensitive to light charged particle, X-rays and gamma rays. Therefore, they offer a very convenient way of detecting heavy ions in the studies of cosmic rays, heavy ion nuclear reactions, and exploration of super heavy elements. These are also most suitable for shielding of devices and in micro filter technology.[5,6] For instance, it is used in preparing track etched membrane to be used as microfilters. Other applications include its use for ion track recording and as packaging material. Similarly, polyethylene terephthalate

(PET) is known for its various applications in capacitors, graphics, recording tapes, etc. It offers good design flexibility and is also lighter and sturdier than most other alternatives, particularly glass.

Passage of SHI in these materials creates large-scale lattice defects due to radiation damage along the path of the ion. This in turns induces the formation and transport of reactive species that are able to permanently change the physical and chemical properties of these solid state nuclear track detectors.[7] Several studies have been performed on the radiation-induced degradation in Makrofol polycarbonate using different kinds of radiations, such as gamma rays,[8] electron beam,[9] neutrons,[10] and heavy ions.[11] Because of the presence of aromatic ring in its polymeric structure, PET has a high melting point and superior mechanical strength. Moreover, it is resistant to heat and moisture, and is virtually nonreactive with many chemicals. Several studies have shown that irradiation of polymers with SHI leads to a wide variety of changes in properties.[12–15] Singh et al.[16] reported a study of electrical and structural properties of PET films irradiated by 50 MeV lithium ions. This investigation aims at studying the effects of Ni ion beam irradiation on Makrofol-KG and PET. The chemical structure of Makrofol-KG (a) and PET (b) are given below:

(a)   (b)
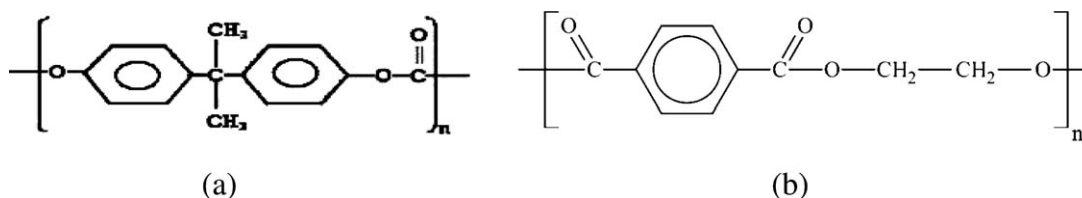
This article compares the irradiation effect of heavier ion at higher energy (120 MeV Ni) on PET and Makrofol-KG. The SRIM calculated range of Ni (120 MeV) for PET and Makrofol-KG are 28.92 μm and 31.21 μm, respectviely.

EXPERIMENTAL

The Makrofol-KG Polycarbonate and PET of thicknesses 40 μm and 100 μm, respectively, were used in this investigation. The polymers films of area 1 × 1 cm² were mounted on a vertical ladder and irradiated with 120 MeV Ni ion beams from the 15 UD Pelletron facilities in Materials Science beam line at Inter University Accelerator Center (IUAC), New Delhi. Fluences ranging from 1×10^{10} to 1×10^{12} ions/cm² were used for irradiation. FTIR spectra were measured by Nexus 670 FT-IR system, which scan the infrared spectrum in the range of 4000–400 cm⁻¹. The XRD studies were carried out by CuKα radiation (λ = 1.54 Å) using Bruker D8 advance from a wide range of Bragg's angle 2θ (5 < 2θ < 40). UV–visible Spectra were obtained using a U-3300 Spectrophotometer. Atomic force microscopy (AFM) was carried out using DI Nanoscope IIIa in tapping mode for studies of surface morphology. The measurments were performed in tapping mode and scanning range was set at 5 μm × 5 μm size in the ambient atmosphere.

RESULTS AND DISCUSSION

X-ray diffraction

The XRD patterns of pristine and Ni^{+9} ion beam irradiated Makrofol-KG and PET are shown in Figure 1. In case of the pristine sample of Makrofol-KG, a strong peak was observed at 2θ = 17.36°, showing the semi crystalline nature Makrofol-KG. After irradiation with Ni^{+9} ions, the intensity of the peak drops sharply. This shows that the polymer crystallinity decreases with increasing fluence and undergoes amorphization.

PET displays similar trends under irradiation. Pristine PET shows a strong peak at 2θ = 25.94° and a weak peak at 2θ = 23.46°. After irradiation, peak intensity is found to decrease with increasing fluences, but no significant shift of peak position is observed. This implies that the lattice parameter

does not change significantly.[17] This may be due to degradation and range of SHI in polymers. The crystallite size of the virgin and irradiated polymer has been calculated using Scherrer's equation[18]:

$$b = K\lambda/L\cos\theta$$

where, b is full width at half maxima in radians, λ is the wavelength of X-ray beam (1.5418 Å), L is the crystallite size in Å, and K (= 1 for polymer) is the Scherrer constant. The above equation was used to calculate the crystallite size (Table I). Nouh et al.[19] studied the effect of electron beam in Makrofol
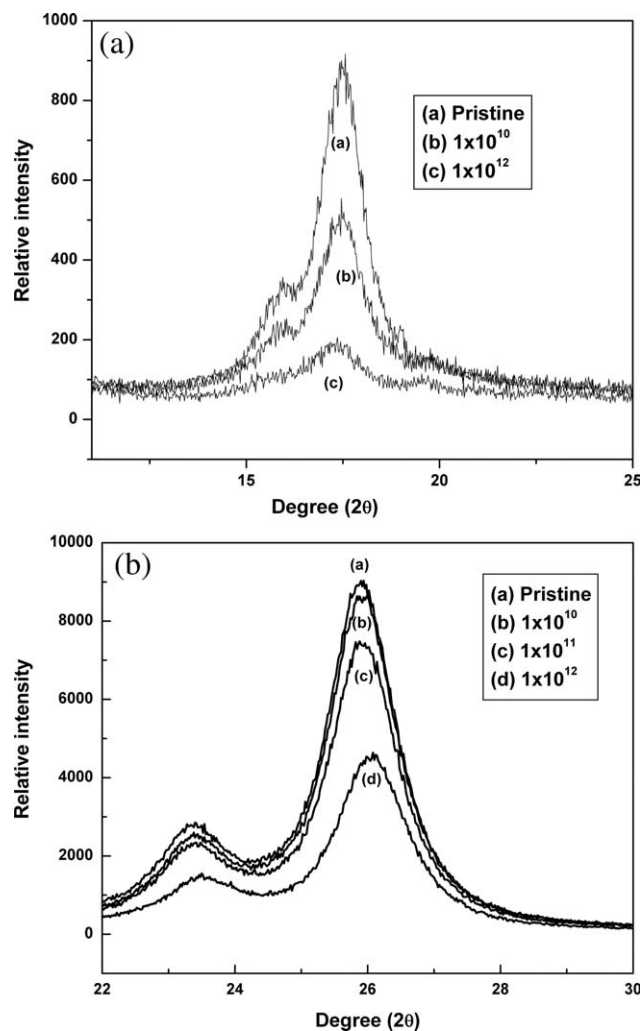

Figure 1 XRD pattern of pristine and Ni beam irradiated (a) Makrofol-KG and (b) PET.

TABLE I
Crystallite Size of Makrofol-KG and PET Polymers Irradiated by 120 MeV Ni Beam

Ni^{+9} ion fluences (Ions/cm^2)	Crystallite size of Makrofol-KG (Å)	Crystallite size of PET (Å)
Pristine	52.9	67.7
1×10^{10}	45.9	63.1
1×10^{12}	37.7	59.9

detector and observed that the degree of ordering of Makrofol is dependent on the electron dose due to degradation and cross-linking processes. The amorphous behavior can be seen in broading of the polymer peak and decrease in the intensity of peak. Similar findings have been reported in other studies. Kumar et al.[20] subjected Polyether Sulphone to heavy irradiation by 70 MeV C^{+5} ions and observed a reduction in the crystallite size. Biswas et al.[21] irradiated PET with Ag^{+14} ions of energy 180 MeV and found that crystallinity decreases with increasing fluence.
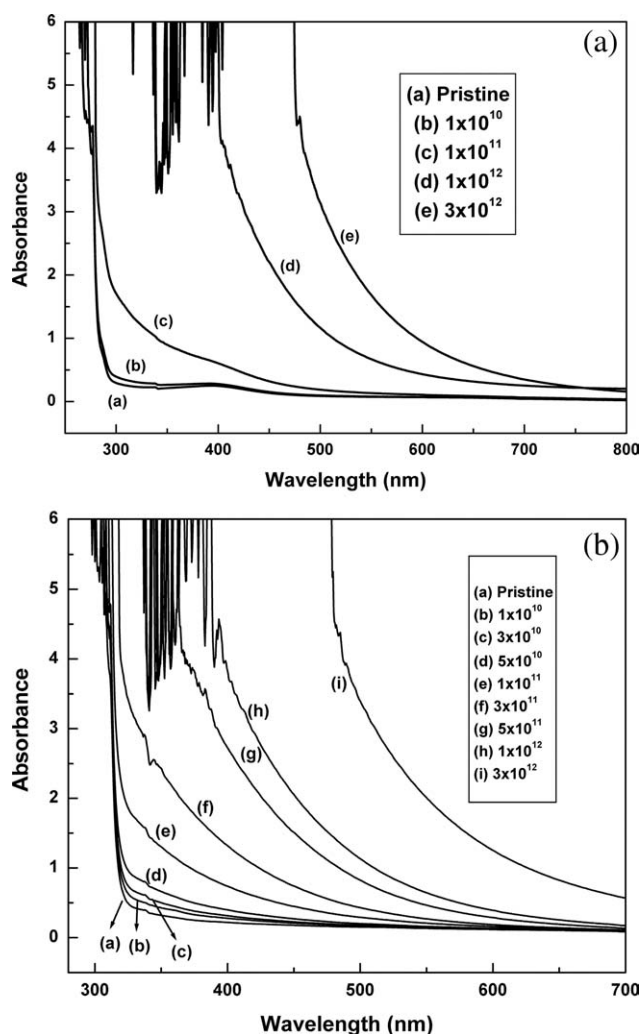

Figure 2 UV–visible spectra of pristine and Ni beam irradiated (a) Makrofol-KG and (b) PET.

UV–visible spectral analysis

The UV–visible spectra recorded for the Ni^{+9} ion beam irradiated polymers displayed in Figure 2 clearly shows a shift in the absorption edge toward longer wavelength with increasing fluencies. This indicates that there is a decrease in band gap after SHI irradiation, which in turns gives rise to the conductivity of the polymer. This shift in the absorption edge may be due to creation of free radicals and molecules during irradiation with highly energetic heavy ions. This may have leaded an increase in the conductivity of the polymers.[22] For this experiment, from the absorption, direct and indirect band gap of the polymers were calculated by linear part of Tauc's plot.[23] The direct and indirect band gaps calculated for pristine Makrofol-KG was found to be 4.1 eV and 3.9 eV, which after irradiation with Ni beam dropped to 1.9 eV and 1.6 eV, respectively (Table II). Similarly, the direct and indirect band gaps calculated for the pristine PET were 3.8 eV and 3.7 eV which after irradiation dropped to 2.3 eV and 1.8 eV, respectively. It may be due to the higher rate of electronic energy loss of 120 MeV Ni beams in polymer, which affects the optical properties of the polymer. It has also been observed that after irradiation, with subsquent evolution of hydrogen or other volatile components the sample become carbon rich.[24] Kulshrestha et al.[25] irradiated PET with SHI and found that the shift of absorption edge was toward longer wavelength. Ramola et al.[26] irradiated CR-39 polycrabonate with O^{+7} ion beam and observed that after irradiation the band gap decreases with increasing fluence. Kumar et al.[27] irradiated Makrofol with Si ion beam and found that after irradiation dielectric constant increases with increasing fluence.

FTIR studies

FTIR spectral analysis was carried out to investigate the structural changes induced in the polymers due to SHI irradiation. The changes were estimated from the relative increase or decrease in

TABLE II
Direct and Indirect Band Gap Variations of Makrofol-KG and PET Polymers Irradiated by 120 MeV Ni Beam

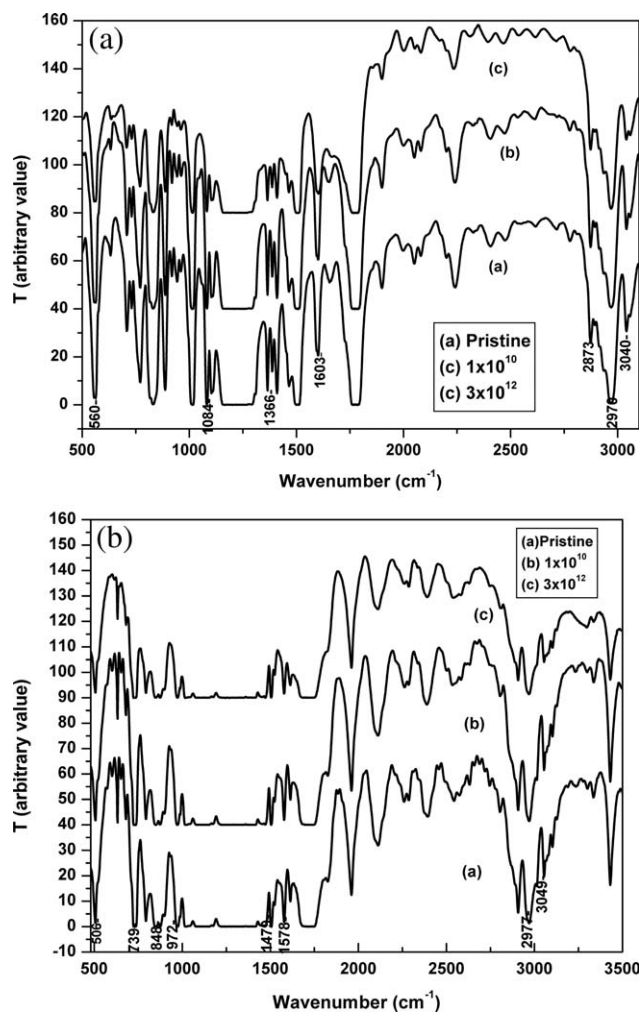| Ni^{+9} ion fluences (Ions/cm^2)	Band gap in Makrofol-KG		Band gap in PET	
	Direct (eV)	Indirect (eV)	Direct (eV)	Indirect (eV)
Pristine	4.1	3.9	3.8	3.7
1×10^{11}	3.0	2.5	3.5	3.4
5×10^{11}	–	–	2.9	2.4
1×10^{12}	2.2	1.8	2.6	2.1
3×10^{12}	1.9	1.6	2.3	1.8

Figure 3 The FTIR spectra of pristine and Ni beam irradiated (a) Makrofol-KG and (b) PET.

the intensity of the peak associated with the functional groups present in the polymers. Figure 3(a) shows the FTIR spectra of pristine and irradiated Makrofol-KG. The observed bands at 2970 cm^{-1},

TABLE III
Wave Number or Functional Group for PET

S. No.	Wave number (cm^{-1})	Functional group
1.	1740 and 730	Stretching vibration of the $C=O-O-$ Ester group
2.	848, 972 and 1472	Trans configuration of ethylene glycol
3.	1503	Skeletal C=C in plane stretching vibration.
4.	2977	Symmetric stretching of $-C-H-$
5.	2872 and 2951	Symmetric and Asymmetric stretching vibration of the CH2 group of ethylene, respectively
6.	3049	$=C-H$ stretching vibration of benzene ring[27]
7.	1176	$C-O-C$ stretching of ester
8.	506	Methylene group

2873 cm^{-1}, and 1366 cm^{-1} corresponds to methyl ($-CH_2$) group and at 3040 cm^{-1}, 1603 cm^{-1}, 1084 cm^{-1}, 560 cm^{-1} corresponds to the para-substituted phenyl.[28] It was observed that after irradiation with 120 MeV Ni ions, the peak intensity decreased with increasing fluence. Figure 3(b) shows the FTIR spectra of virgin and irradiated PET polymer film. The virgin PET film is characterized by strong bands at 730 cm^{-1} representing the stretching vibration of the ($-COOR$) ester group, at 506 cm^{-1} representing methylene group, at 848 cm^{-1} and 972 cm^{-1} for ethylene glycol. The absorption band at 2977 cm^{-1} is assigned for symmetric stretching[29] of $-CH-$. Some other bands[28–32] that appeared in the spectra are summarized in Tables III and IV. Here again it was observed that after irradiation, the peak intensity decreased with increasing fluences. The observed decrease in intensity in the different bands can be attributed to the fact that energy lost by SHI may have been used for many processes, such as amorphization of the crystalline fraction of the polymer, scission of the chains and oxidation.[33–35] Singh et al.[16] irradiated Makrofol detector with proton ion and found that at higher fluence the peak intensity decreases. Drabik et al.[36] observed that there was an overall decrease of intensity of typical bands in PET after irradiation with SHI.

AFM studies

In this investigation, AFM was performed to examine the surface morphology and to measure roughness value for pristine and irradiated Makrofol-KG and PET films irradiated at different fluences. Figures 4 and 5 show the three-dimensional topographic scan of (pristine and irradiated) Makrofol-KG and PET, respectively. It was found that the surface of pristine polymers was smooth and that after irradiation the roughness increased with increasing fluence. This increase in roughness of polymer surface is related to the progressive degradation of the polymeric chains due to intermolecular cross-linking, leading to changes in free volume fraction of the modified surface layer.[37]

TABLE IV
Wave Number or Functional Group for Makrofol

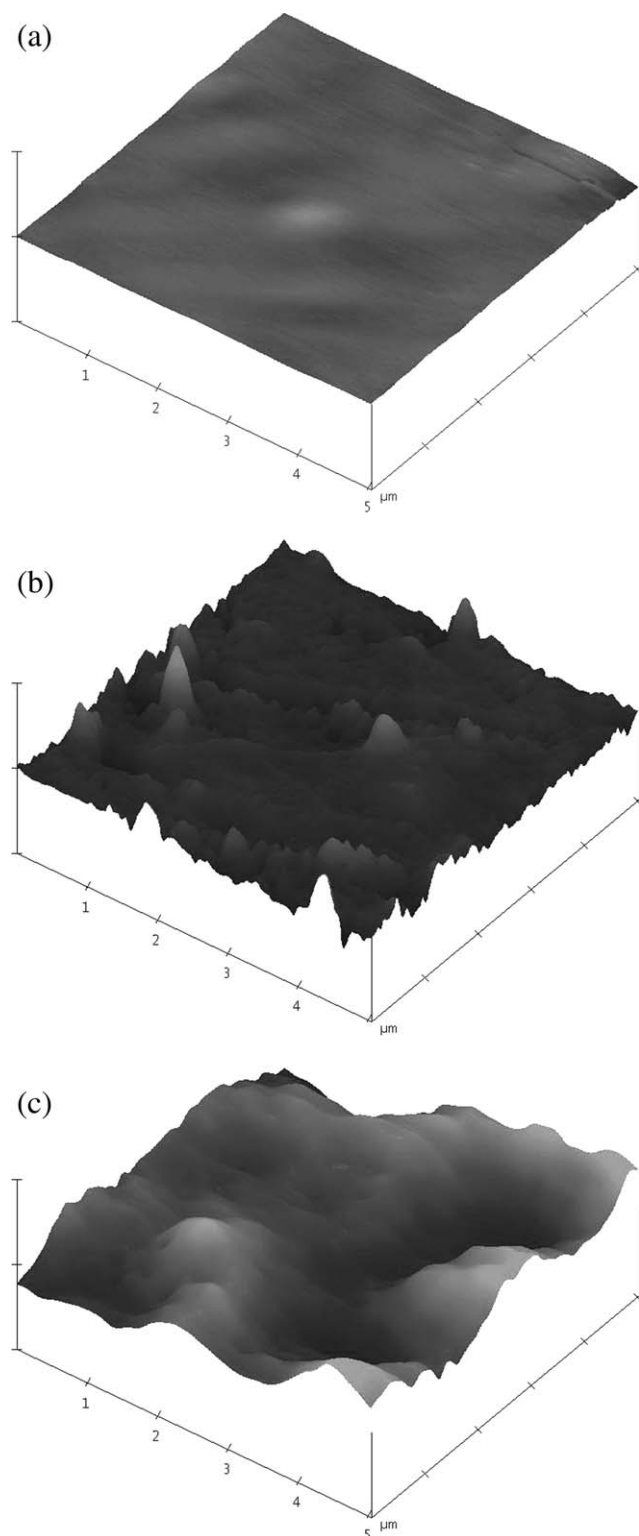| S. No.	Wave number (cm^{-1})	Functional group
1.	3040, 3060, 1603, 1504, 1084, 1017, and 833	Para-Substituted Phenyl group
2.	2970, 2873, 1467, 1366, 1388	Methyl group
3.	1770	($-C=O$) stretching band
4.	1220 and 889	Asymmetric stretching of the aromatic ether and symmetric stretching

(a)

and subsequent creation of free radicals that initiate the modifications as well as the formation of chemical bonds between different molecules/chains (intermolecular cross-linking). The consequent disorder in the systems on account of all these processes can be regarded as a loss of crystallinity. The decrease in
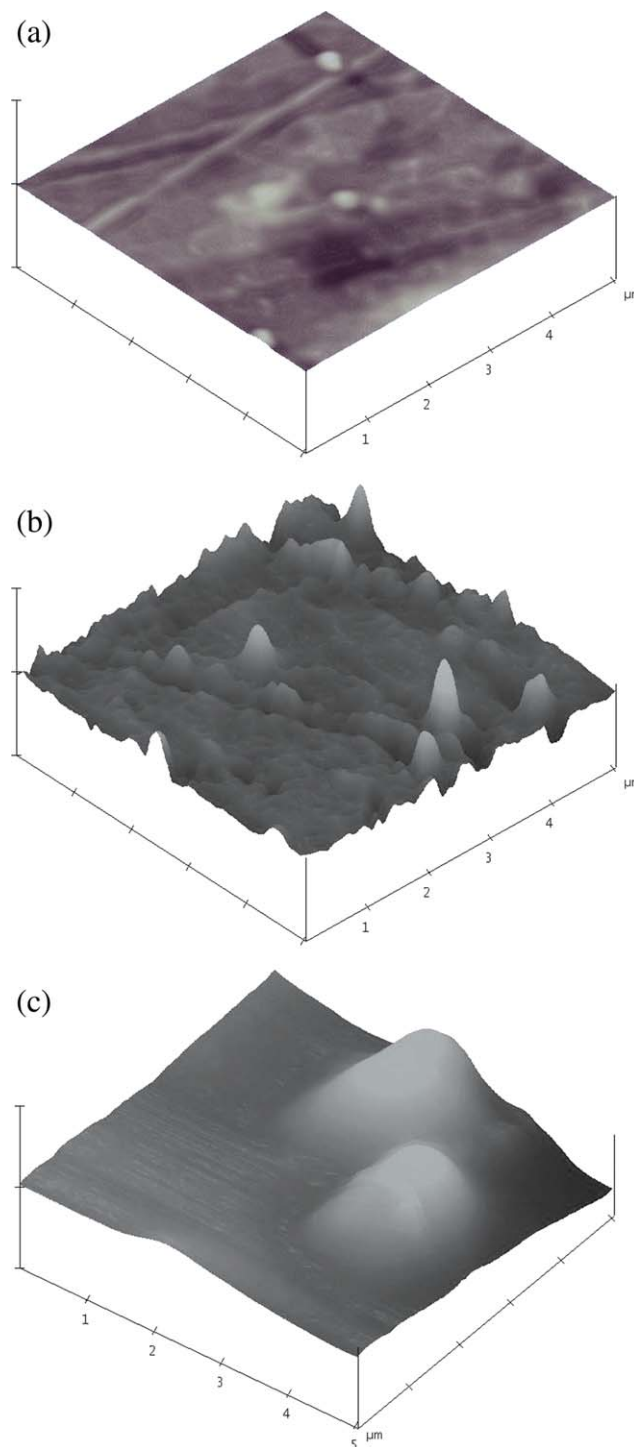
(a)

(b)

(b)

(c)

Figure 4 AFM Scan Makrofol-KG for (a) pristine and irradiarted with Ni beam of fluence (b) 1×10^{10} and (c) 1×10^{12} ions/cm^2.

CONCLUSIONS

The chemical changes induced by dense ionizing radiation in polymer involve several processes such as cleavage of bonds (scission) in the main chain

(c)

Figure 5 AFM Scan PET for (a) pristine and irradiarted with Ni beam of fluence (b) 1×10^{10} and (c) 5×10^{11} ions/cm^2. [Color figure can be viewed in the online issue, which is available at wileyonlinelibrary.com.]

the crystallite size of the polymer after irradiation with high-energy heavy-ion beam and with the increasing fluence appears to be due to the degradation of the polymer by scissioning. This finding is in agreement with the XRD results where it was found that amorphization takes place and it increases with increasing fluence. Decrease in the intensity of the bands and small increase in the broadening peak in FTIR spectra can be attributed to the degradation mechanism like preferential chain scissioning and cross linking, respectively. The influences of high-energy heavy-ion irradiation on optical, structural and morphological changes of the Makrofol-KG and PET were investigated using 120 MeV Ni beam. The UV–visible spectra demonstrated a decrease in the band gap along with a shift in the peak with increasing ion fluences. The XRD revealed a decrease in crystallinity with increasing fluence. Surface topography of the pristine and irradiated polymer samples showed that after irradiation roughness increases with increasing fluences. All these changes have been attributed to the fact that SHI induces chain scissioning, formation of free radicals and subsequent cross-linking of the polymer chains.

References

1. Adle, A.; Buschmell, V.; Fuess, H.; Trautmann, C. Nucl Instrum Methods Phys Res 2001, 185, 210.
2. Venkatesan, T. Nucl Instrum Methods Phys Res B 1985, 461, 7.
3. Dole, M. The Radiation Chemistry of Macromolecules, Vol. 1; Academic Press: New York, 1972.
4. Dole, M. The Radiation Chemistry of Macromolecules, Vol. 2.; Academic Press: New York, 1973.
5. Fleischer, R. L.; Price, P. B.; Walker, R. M. Nuclear Tracks in Solids. Principles and Applications; University of California Press: Berkeley, 1975.
6. Durrani, S. A.; Bull, R. K. Solid State Nuclear Detection; Pergamon Press: Oxford, 1987.
7. Mishra, R.; Tripathy, S.; Dwivedi, K.; Khathing, D.; Ghos, S.; Muller, M.; Fink, D. Radiat Meas 2003, 37, 247.
8. Sinha, D.; Dwivedi, K. Radiat Meas 2003, 40, 50.
9. Seguchi, T.; Yagi, T.; Ishikawa, S.; Sano, Y. Radiat Phys Chem 2002, 63, 35.
10. Ranby, B.; Rabek, J. ESR Spectroscopy in Polymer Research, Vol. 9; Springer: Berlin, 1997; p 607.
11. Ferrain, E.; Legras, R. Nucl Instrum Methods Phys Res B 1993, 825, 39.
12. Srivastava, A.; Singh, T.; Sharma, S. M.; Ranjan, C. R.; Ponrathnam, S. Nucl Instrum Methods B 2002, 192, 402.
13. Srivastava, A.; Singh, T.; Sharma, A. L.; Janin, P. K.; Rajan, C. R.; Ponrathnam, S. Radiat Eff Defects Solids 2003, 158, 561.
14. Sonar, P.; Sharma, A. L.; Chandra, A.; Mullen, K.; Srivatava, A. Curr Appl Phys 2003, 3, 247.
15. Singh, S.; Prasher, S. Nucl Instrum Methods Phys Res B 2006, 244, 252.
16. Singh, N. L.; Shah, N.; Singh, K. P. Bull Mater Sci 2005, 28, 599.
17. Wang, Y.; Jin, Y.; Zhu, Z.; Liu, C.; Sun, Y.; Wang, Z.; Hou, M.; Chen, X.; Zhang, C.; Liu, J.; Li, B. Nucl Instrum Methods Phy Res B 2000, 164, 420.
18. Patterson, A. L. Phys Rev 1939, 56, 978.
19. Nouh, S. A.; Ibrahim El-Tayeb, N.; Said, A. F.; Radwan, M. M.; EL-Fiki, S. A. Radiat Meas 2007, 42, 8.
20. Kumar, R.; Deand, U.; Pradas, R. Nucl Instrum Methods Phys Res B 2006, 248, 279.
21. Biswas, A.; Lotha, S.; Fink, D.; Singh, J. P.; Avasthi, D. K.; Yadav, B. K.; Bose, S. K.; Khating, D. T.; Avasthi, A. M. Nucl Instrum Methods Phys Res B 1999, 159, 40.
22. Singh, S.; Prasher, S. Nucl Instrum Methods Phys Res B 2004, 222, 518.
23. Tauc, J.; Grigorovici, R.; Vancu, A. Phys State Solid B 1966, 15, 627.
24. Prakash, J.; Tripathi, A.; Khan, S. A.; Singh, F.; Tripathi, J.; Kumar, S.; Avasthi, D. K. Vacuum 2010, 84, 1275.
25. Kulshrestha, V.; Awasthi, K.; Acharya, N. K.; Singh, M.; Bhagwat, P. V.; Vijay, Y. K. Polym Bull 2006, 56, 427.
26. Ramola, R. C.; Chandra, S.; Rana, J. M. S.; Sonkawade, R. G.; Kulerya, P. K.; Singh, F.; Avasthi, D. K.; Annapoorni, S. J Phys D Appl Phys 2008, 41, 115411.
27. Kumar, R.; Singh, P.; Ali, S. A.; Sharma, A.; Khan, S. A.; Sonakawede, R. G.; Pradas, R. Indian J Pure Appl Phys 2010, 48, 166.
28. Sun, Y.; Zhu, Z.; Wang, Z.; Jin, Y.; Liu, J.; Zhang, M. Q. Nucl Instrum Methods Phys Res B 2003, 209, 188.
29. Singh, V.; Singh, T.; Chandra, A.; Bandyopadhyay, S. K.; Sen, P.; Witte, K.; Scherer, U. W.; Srivastava, A. Nucl Instrum Methods Phys Res B 2006, 244, 243.
30. Nasef, M. M. J Appl Polym Sci 2002, 84, 1949.
31. Takahashi, S.; Yoshida, M.; Asano, M.; Nakagawa, M. T. Nucl Instrum Methods Phys Res B 2004, 217, 435.
32. Dworecki, K.; Hasegawa, T.; Suditz, K.; Wasik, S. Nucl Instrum Methods Phys Res B 2000, 166–167, 646.
33. Steckenreiter, T.; Balazat, E.; Fues, H.; Trautmann, C. Nucl Instrum Methods Phys Res B 1997, 131, 159.
34. Silverstein, R. M.; Bassler, G. C.; Morill, T. C. Spectrometric Identification of Organic Compounds; Wiley: New York, 1990.
35. Ciesla, K.; Starosta, W. Nucl Instrum Methods Phys Res B 1995, 105, 115.
36. Drabik, M.; Dworecki, K.; Tanczyk, R.; Wasik, S.; Zulk, J. Vacuum 2007, 81, 1348.
37. Nathawat, R.; Kumar, A.; Kulshrestha, V.; Vijay, Y. K.; Kobayashi, T.; Kanjilal, D. Nucl Instrum Methods Phys Res B 2008, 266, 47.